

Nanoscale

Accepted Manuscript



This is an *Accepted Manuscript*, which has been through the Royal Society of Chemistry peer review process and has been accepted for publication.

Accepted Manuscripts are published online shortly after acceptance, before technical editing, formatting and proof reading. Using this free service, authors can make their results available to the community, in citable form, before we publish the edited article. We will replace this *Accepted Manuscript* with the edited and formatted *Advance Article* as soon as it is available.

You can find more information about *Accepted Manuscripts* in the [Information for Authors](#).

Please note that technical editing may introduce minor changes to the text and/or graphics, which may alter content. The journal's standard [Terms & Conditions](#) and the [Ethical guidelines](#) still apply. In no event shall the Royal Society of Chemistry be held responsible for any errors or omissions in this *Accepted Manuscript* or any consequences arising from the use of any information it contains.

Chemically modified diamondoids as biosensors for DNA

Ganesh Sivaraman and Maria Fyta*

*Institute for Computational Physics, Universität Stuttgart, Allmandring 3, 70569 Stuttgart,
Germany*

E-mail: mfyta@icp.uni-stuttgart.de

Abstract

Understanding the interaction of biological molecules with materials is essential in view of the novel potential applications arising when these two are combined. To this end, we investigate the interaction of DNA with diamondoids, a broad family of tiny hydrogen-terminated diamond clusters with high technological potential. We model this interaction through quantum-mechanical computer simulations and focus on the hydrogen bonding possibilities of the different DNA nucleobases to the lower amine-modified diamondoids with respect to their relative distance and orientation. Our aim is to promote the binding between these two units, and probe this through the association energy, the electronic structure of the nucleobase-diamondoid system, and the specific role of their frontier orbitals. We discuss the relevance of our results in view of biosensing applications and specifically nanopore sequencing of DNA.

Introduction

DNA carries the genetic information of all living organisms. In this respect, a lot of efforts have turned into novel biotechnological applications which could sense biomolecules, such as DNA,

*To whom correspondence should be addressed

and read-out efficiently the information therein. One of the promising candidate for a future label free DNA sequencing technology is a nanopore based DNA sequencer.¹⁻³ In this technique a single-stranded DNA molecule is translocated through a nanometer-sized pore by electric means. Transverse current measurements can lead to the identification of the nucleotide sequence, for which the signal-to-noise ratio is still too low. The biosensing properties of the nanopore, though, could be enhanced through functionalization of the nanopore.^{1,4} The specific interaction of the functionalizing molecule with the DNA units has the potential to reduce the noise in the transport measurements.⁵ It is thus important to search for a molecule, which could specifically bond to each DNA nucleobase and lead to distinct signals. These molecules should be comparable in size to the nucleobases and compatible with electronics.

Candidates for this purpose are diamondoids.⁶ These are tiny hydrogen-terminated diamond cage-like structures, which have shown strong potential for nanotechnological⁷⁻⁹ and pharmaceutical applications.^{10,11} Some of the derivatives of the lower diamondoid, adamantane, such as amantadine, memantine, and rimantadine,¹² have found applications as anti-viral¹³ and anti-Parkinsons agents.¹⁴ Studies have shown that the amine substituted lower diamondoids develop good conductance properties depending on their relative orientation between two electrodes¹⁵ and have good electron emission properties.^{8,16} Thiol groups have also been proposed to be very good candidates for functionalizing diamondoids, in order to attach them to nanoscale devices.^{17,18}

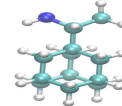
The goal of our work is to exploit the hydrogen bonding possibility of diamondoids with nucleobases, as well as the semiconducting properties of the diamondoid-nucleobase complex along the hydrogen bonded orientations to enhance future tunneling current measurements for sensing DNA. As a first step in studying the feasibility for a diamondoid to sense DNA, we seek the bonding characteristics of a diamondoid placed close to a DNA nucleobase and investigate the strength of the resulting hydrogen bond, as well as its dependence on the relative distance and orientation of the two molecules. The choice of a diamondoid as a probe for sensing DNA is based on the variability in sizes and the various modification possibilities it offers,¹⁹ as well as the ease in chemically attaching these onto the edge of nanopore, an issue we will discuss again in the Conclusion

Section.

Methodology

We perform computer simulations for different diamondoid-DNA nucleobase complexes. In this way, we probe the binding characteristics of these two entities, the diamondoid and the nucleobase. Bonding of a diamondoid to all four nucleobases, adenine (A), thymine (T), cytosine (C), and guanine (G) is studied. In order to promote bonding we choose derivatives of the smallest diamondoid, adamantane.¹² We begin with three derivatives of adamantane, amantadine ("ama"), memantine ("mem"), and rimantadine ("rim"). The first two have one of their sites substituted by an amine group, while the third one has one of its sites substituted by an ethanamine group. These are all sketched in Table 1. The reason for these choices is first computational efficiency and second that we would like to probe the biosensing possibilities of a small molecule relative in size with the DNA nucleobases. We next combine each of the three diamondoid derivatives with one of the four nucleobases. All the possible conformations for interaction are chosen in a way that the amine group of the diamondoid acts as a hydrogen bond acceptor for the nucleobases. Here, we scan a finite part of the conformational space of these two entities, as it is not possible to include the whole conformational space in our quantum mechanical calculations. Our aim though is to present a proof of principles regarding the binding possibilities of diamondoids and DNA nucleobases and not to provide a thorough scan of their different conformations.

Table 1: Amine-derivatives of adamantane

memantine	amantadine	rimantadine
$C_{12}H_{21}N$	$C_{10}H_{17}N$	$C_{12}H_{21}N$
		

Our calculations are based on density functional theory (DFT) and have been performed using the code SIESTA.²⁰ We use norm-conserving Troullier-Martin pseudopotentials²¹ and a split

valence triple zeta polarized basis set.²² A mesh cutoff parameter (which corresponds to the fineness of the real space grid) of 250 Ry has been found to be optimal for the calculations. We have been using the exchange-correlation functional VDW-DF2.²³ Due to the explicit inclusion of a strictly non local correlation term, this functional is found to describe dispersion interactions with improved accuracy in comparison to a semi-local generalized-gradient-approximation (GGA) functional.²⁴ The pseudopotentials, the basis set, and the VDW-DF2 functional were benchmarked with respect to the geometry and binding energy of Adenine-Thymine Watson-Crick base pairs.²⁵ The geometry optimization was performed using the conjugate gradient algorithm and the structure was relaxed until the forces acting on the atoms were lower than 0.04 eV/Å. The benchmarking results were in excellent agreement with previous calculations.²⁶ The interaction energy is calculated as the difference between the total energy of the geometry-optimized hydrogen bonded complex with that of isolated monomers in the gas phase. The results have been corrected for the basis set superposition error (BSSE)²⁷ without a geometry distortion correction. This choice was based on the comparison of our results to those of known nucleobase complexes in the literature.^{25,26}

Results and discussion

We next present the main outcome of our investigation and begin our analysis by investigating the strength of the hydrogen bond. We should first note that for all the diamondoid-nucleobase complexes we have studied, there is at least one non-negligible hydrogen bond that forms and connects the two components, diamondoid and nucleobase.

Association energy

The association energy for individual hydrogen bonded complexes is summarized in Table 2. The association energy is the hydrogen bond energy denoting the strength of the hydrogen bond. The association energy is defined as the total energy of the complex subtracted by the total energy

of the two isolated components, nucleobase and diamondoid. The total energy is the energy as obtained through the DFT calculations. The bond-length and bond-angle for the geometry optimized structure is shown in Table 3 with respect to the amine group hydrogen bond acceptor site of the diamondoid. The hydrogen bond-angle is usually in the range of 140 – 180 deg.. At angles closer to planar the interaction is expected to be electrostatic. At larger angles, the interaction is dispersion driven. Note also that hydrogen bonding can be classified according to the interaction strength, i.e. association energies (E_{assoc}) as:^{28,29} (i) strong [$E_{assoc} > 15$ kcal/mol(0.65 eV)], (b) moderate [$E_{assoc} \approx 4$ -15 kcal/mol(0.17-0.65 eV)], and weak [$E_{assoc} < 4$ kcal/mol(0.17 eV)].

Table 2: Association energy of hydrogen-bonded complexes.

Association energy E_{assoc} [kcal/mol, (eV)]			
System	memantine	amantadine	rimantadine
adenine	-8.978(-0.3893)	-9.306(-0.4035)	-9.298(-0.4032)
thymine	-10.228(-0.4435)	-10.198(-0.4424)	-9.972(-0.4324)
guanine	-11.711(-0.5078)	-11.719(-0.5082)	-10.290(-0.4462)
cytosine	-12.122(-0.5250)	-11.609(-0.5034)	-11.328(-0.4912)

Inspection of Table 2, clearly reveals that all the hydrogen bonds of the diamondoid-nucleobase complexes are of moderate strength and lie between 9 – 12(0.38-0.52) kcal/mol(eV). It is also evident from Table 3, that for the hydrogen bonded complexes formed by memantine and amantadine the hydrogen bond-angle is closer to planar. For the complexes formed by rimantadine (except for the rimantadine-guanine complex) the bond angle is lower in comparison to the other complexes. We base this difference on the fact that the hydrogen atoms in the amine group of rimantadine need to rearrange, so that the amine group can act as a hydrogen bond acceptor. On the other hand, a minimal rearrangement is required in the case of the amantadine and memantadine complexes. As can be inspected from Fig. 1 for the chosen initial configuration of these complexes, the amine group readily accepts the hydrogen from the donor site of the adjacent nucleobase resulting in angles close to planar. Note, that in all cases the hydrogen bond-lengths are in the range of $\approx 3.0 - 3.2$ Å.

Table 3: Bond-length (donor-acceptor distance in Å) and bond-angle (donor-hydrogen-acceptor angle in degrees) of the hydrogen-bonded complexes.

	bond-length(bond-angle) Å(deg.)		
System	memantine	amantadine	rimantadine
adenine	3.080(169.6)	3.106(174.4)	2.996(147.8)
thymine	3.122(171.4)	2.993(174.23)	2.918(152.5)
guanine	3.190(175.6)	3.171(169.6)	3.200(169.7)
cytosine	3.061(179.2)	3.06(178.4)	3.071(146.5)

Orientation and distance dependence

An additional important indication of the hydrogen bond strength is its deviation with respect to the diamondoid-nucleobase optimized geometry as predicted from the DFT calculations. This we define as the *optimized geometry* and serves as a reference for comparison. This reference is needed, as in real applications a nucleobase may approach the diamondoid at orientations and distances different from the ideal scenario, which is studied using the DFT optimized geometry. In the following, we will characterize the distance and orientation dependence of the hydrogen bond for all diamondoid-nucleobase complexes. For this we present our results with respect to the distance between the amine group hydrogen-bond donor of the diamondoid to the acceptor group of the nucleobase (the distance is defined between the two N atoms involved in this bond). The N–N donor-acceptor axis denotes the axis along which the geometry optimization was done. We also define a propeller angle for the relative orientation of the diamondoid with respect to the nucleobase. The propeller angle rotation axis is defined by two carbon atoms. The one is the carbon atom on the nucleobase site which defines one end of the propeller axis and has been chosen according to similar studies found in the literature.²⁶ The second C atom on the diamondoid end has been chosen to belong to the rigid cage structure of diamondoid. It is the site of the diamondoid which is in plane with the nucleobase and can be directly or through a thiol group be attached on a surface of a biosensing device. The N–N and propeller (C–C) axes about which the nucleobase was rotated with respect to a fixed diamondoid can be seen in Fig. 1 for the amantadine-nucleobase complexes. These axes are exactly equivalent for the complexes formed by the other two diamondoids.

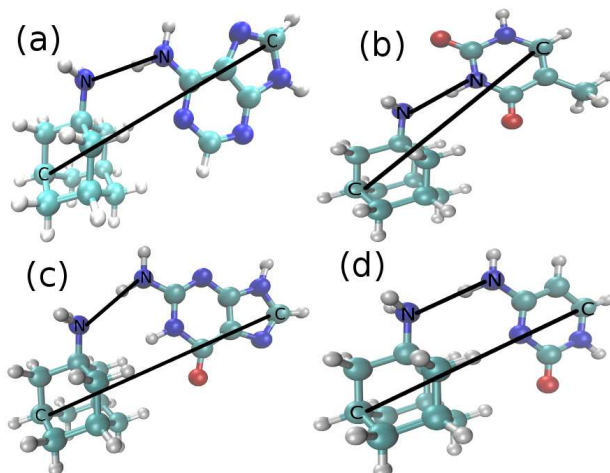


Figure 1: The N–N donor acceptor axis denotes the axis along which the geometry optimization was done. The C–C axis denotes the propeller angle rotation axis (see text for definitions). The conformations correspond to the initial configurations chosen for our simulations for the (a) ama-A, (b) ama-T, (c) ama-G, and (d) ama-C complexes, respectively.

We begin with an optimized geometry as a reference for which the propeller angle is defined as 0 degrees. We then vary the distance between the two units of the complex, the diamondoid and the nucleobase, and summarize the results in Fig. 2. This figure shows the variation of the association energy (E_{assoc}) with respect to this distance for all complexes studied in this work. It is obvious that all energies lie in the same moderate range as mentioned previously for the optimized cases (see Table 2). For the same nucleobase the association energy minimum corresponds to the same distance. This does not hold only for the case of the memantine-T complex for which the minimum is shifted towards higher distances compared to the other T-complexes. A further analysis of this result has been done in one of the following section in which the frontier orbitals of the complexes are analyzed.

We next take as the reference the optimized complexes, i.e. the ones who correspond to the association energy minima in Fig. 2 in order to unveil the rotational dependence of the hydrogen bonding in the diamondoid-nucleobase complexes. This dependence is studied by rotating the

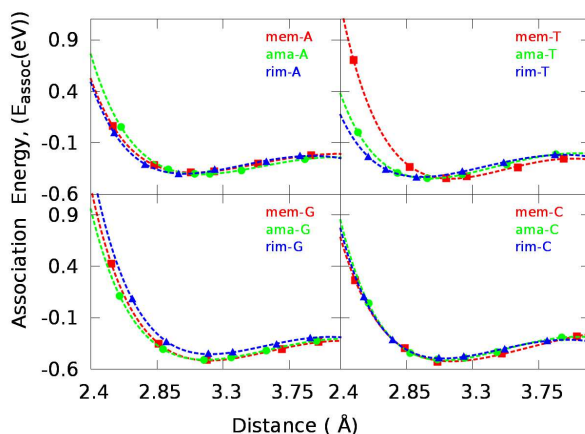


Figure 2: Association energy (E_{assoc}) as a function of the diamondoid-nucleobase distance.

nucleobase along the C–C axis shown in Fig. 1. The results can be reviewed in Fig. 3 for all diamondoid-nucleobase complexes studied here. In this graph, the deformation energy is shown, i.e. the energy difference between the complex in which the nucleobase has been rotated and the optimized reference structure of the same complex. It is clearly evident that when the donor group of the nucleobase approaches the amine acceptor group of the diamondoid at larger angles the dispersion forces increase, thus the interaction and the deformation energy increases. An exception was found in the case of the ama-T complex in which the interaction remains strong, i.e. the deformation energy goes to zero even at large negative propeller angles. This is justified by the observation that for all negative propeller angles, a very small deviation in the donor-hydrogen-acceptor angle was observed. Note, that for positive propeller angles, the deformation energy again increases as in all other complexes. For these angles, a change in the donor-hydrogen-acceptor angle is now evident. One interesting observation is that for the cytosine interaction with memantine, at larger angles, the interaction becomes weak (the deformation energy increases) with respect to that of the geometry optimized hydrogen bonded reference structure. In this case, as the absolute value of the propeller angles increase, the conformation of the complex deviates significantly from the reference, i.e. the conformation of stronger coupling between memantine and cytosine. For all other cases, the interaction is found to be moderate again with respect to the

reference structure.

A comparison of all complexes reveals that the deviation from the optimized reference geometry is non-monotonic. This behavior is based on the fact that the rotation along the C–C axis in each complex is not symmetric for positive and negative propeller angles. This occurs mainly because the hydrogen bond angles (shown in Table 3) are non planar. Two exceptions occur for the mem-C and ama-C cases, which are almost symmetric, as the hydrogen bond angles of their reference conformations are almost planar. Overall, no conclusion can be drawn whether this deviation is stronger for one of the diamondoids in any complex. This is again evident from Fig. 3 where the energy for the mem-A complex shows a smaller increase compared to the mem-G case, which probably reflects larger deviations from the reference structure for larger angles for the latter case. The behavior of the other complexes is similar. Note, that we have focused on the one strong/moderate hydrogen bond that occurs between a diamondoid and a nucleobase, for which the characteristics are given Table 3. This hydrogen bond is expected to lead to enhanced nucleobase-specific tunneling currents in a sensing device. Nevertheless, more than one weak hydrogen bonds have also been observed in all complexes, but for these both the hydrogen bond and hydrogen bond angle are large enough, decreasing significantly the association energy. Hence, the lifetime of these weak hydrogen bonds is expected to be very short to be used in sensing the bases, and are thus not of high interest in this work.

Frontier orbitals and electronic structure

At a final step, the electronic properties of the nucleobase-diamondoid complexes are analyzed. We focus on their frontier orbitals - the highest occupied and lowest unoccupied molecular orbitals, HOMO and LUMO, respectively - as well as their electronic structure as probed through the electronic density of states (eDOS) and the electronic band-gap. We next always refer to the geometry optimized structure of each diamondoid-nucleobase complex. We begin with the analysis on the frontier orbitals and show these for the hydrogen bonded structure of amantadine with all

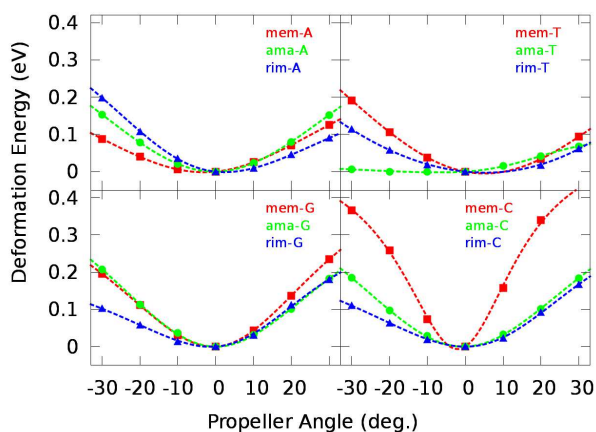


Figure 3: Deformation energy as a function of the propeller angle with respect to the optimized geometry corresponding to the minimum for each diamondoid-nucleobase complex in Fig. 2.

nucleobases in Fig. 4. For all ama-nucleobase complexes both the HOMO and LUMO states are located at the nucleobase site. The HOMO and LUMO orbitals of the complex are associated with the nucleobase only. For comparison, the HOMO and LUMO orbitals for isolated adamantane and adenine molecules are shown in Fig. 5. Comparing panels (a) and (b) in this figure with panel (a) from Fig. 4 reveals that the HOMO, LUMO orbitals of adenine not only dominate in the complex, but are also not altered by the presence of the adjacent adamantane. The HOMO, LUMO states of the isolated adenine are indeed those that correspond to the HOMO and LUMO states of the ama-A complex, respectively.

Similar are the features for some of the mem- and rim- hydrogen-bonded complexes, shown in Fig. 6 and Fig. 7, respectively. The HOMO and LUMO states of the complexes correspond to the HOMO and LUMO states of the nucleobase for the mem-A, mem-G, and rim-G cases. We find a deviation from this observation for the other memantadine and rimantadine complexes, namely rim-A, rim-T, mem-T, rim-C, and mem-C. In these cases, the diamondoid is also associated with the HOMO state of the complex. In the first three cases (i.e. rim-A, rim-T, and mem-T), two are the factors that stabilize the complex, the repulsion between the HOMO state of the nucleobase

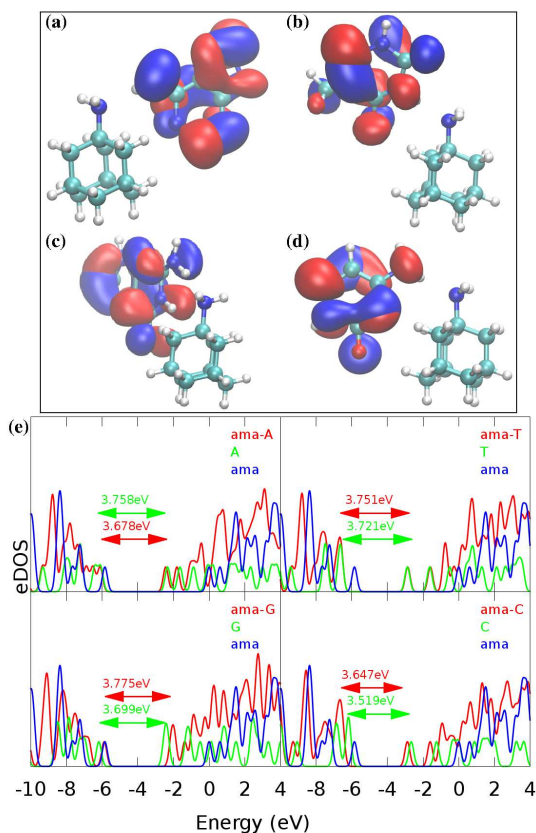


Figure 4: The frontier orbitals, HOMO (blue) and LUMO (red), for the four hydrogen bonded amantadine-nucleobase complexes: (a) ama-A, (b) ama-T, (c) ama-G, and (d) ama-C. In (e) the electronic density of states (eDOS) and band gap for the amantadine-nucleobases complexes are shown. The eDOS in all cases are shifted with respect to the LUMO state of amantadine which is placed at 0 eV.

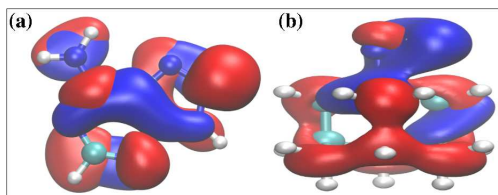


Figure 5: Frontier orbitals for (a) an isolated adenine and (b) an isolated amantadine. The HOMO orbitals are sketched in blue and the LUMO in red.

and that of the diamondoid, as well as the attraction of the LUMO state of the nucleobase with the HOMO state associated with the amine group site of the diamondoid. In the previous section it was observed that the mem-T complex has its energy minima shifted towards higher distances compared to other diamondoid-T complexes. The origin of this comes from a possible compromise between the attractive and repulsive interaction of the frontier orbitals, as well as the fact that the donor-hydrogen-acceptor angles for mem-T are close to planar in comparison to rim-T. Accordingly, the repulsion of the frontier orbitals is reduced by increasing the distance. In the last two cases (i.e. rim-C and mem-C), the HOMO state of the complex is associated solely with that of the diamondoid, while the LUMO state originates only from the nucleobase resulting in hydrogen-bonded complexes which are stabilized by the attraction of these two states. Note, that diamondoid levels which usually populate the HOMO are driven down in about two third of the complexes studied here, and the HOMO and LUMO levels in those cases are solely located on the nucleobase. A possible explanation of this could be a charge transfer between the diamondoid and the nucleobase, which shifts the diamondoid HOMO levels towards lower energies. An additional study to shed more light into this issue is further planned.

In order to understand this and also provide an insight on possible conductance measurements along these complexes, we turn to the electronic density of states (eDOS) of the complexes. These are summarized in Figs. 4(e), 6(e), 7(e), for the ama-, mem-, and rim-nucleobase complexes, respectively. The eDOS for the isolated nucleobases and isolated diamondoids are also given in each panel for comparison. The numbers on the graphs denote the electronic band-gaps of the complexes and isolated nucleobases. The eDOS are shifted with respect to the LUMO state of the isolated diamondoid in each case. This choice was made because the isolated diamondoid is assumed to be the reference for evaluating the electronic properties of the complexes. In a potential biosensing device, the diamondoid will be the sensing probe. It should be underlined, that we are aware of the problem of DFT in calculating correct electronic band gaps. Here, though, we do not care about absolute numbers, but rather aim in comparing the band-gaps for the different complexes and the isolated diamondoids studied. The electronic band-gaps we have obtained

for the isolated diamondoids from our computations are 5.848 eV, 5.829 eV, and 5.719 eV, for amantadine, memantine, and rimantadine, respectively.

Inspection of the eDOS reveals, that in all complexes a part of the band gap region of the isolated diamondoids is filled by the states of the nucleobases. As a general remark, the band-gaps of the hydrogen bonded complex are in comparable range to that of the isolated nucleobases. For all the diamondoid-A complexes the band-gap difference between the complex and the bare nucleobase is about 0.08-0.1 eV, for the diamondoid-T complexes it is 0.03-0.06 eV, and for the diamondoid-G it is 0.06-0.09 eV. We see a large difference between the two diamondoid-C complexes the band-gap differences mentioned above are about 0.12-0.13 eV, but for rim-C this difference rises to 0.36 eV. Similarly the corresponding band gap differences for the rim-T case are about 0.03-0.04 eV larger than in the ama-T and mem-T cases.

The first important implication of these results with respect to biosensing abilities of small modified diamondoids is that rimantadine can be used to clearly distinguish cytosine among all the other nucleobases, and possibly also thymine. Differences in the band-gaps could imply that variations in the transport properties along different diamondoid-nucleobase complexes can potentially also be observed. According to the eDOS data we present here, for a specific diamondoid, the band-gap differences of the complex and the isolated nucleobase are small, but do differ. For example, these differences are 0.08 eV for ama-A, 0.03 eV for ama-T, 0.77 eV for ama-G, and 0.14 eV for ama-C, and are non-negligible. Taking the isolated diamondoids as references will lead to the following band-gap differences between the isolated diamondoids and the A-complexes. These will be 2.09 eV, 2.06 eV, and 1.96 eV for the ama-A, mem-A, and rim-A cases respectively. The respective differences between the band-gaps for isolated diamondoids and the ama-T, mem-T, and rim-T complexes are 2.13 eV, 2.10 eV, and 2.0 eV. Some of these differences are within the error, but differences do exist. We should note here, that in a biosensing device, either it is a nanopore or a surface on which a diamondoid is attached and should sense DNA molecules, a salt solution will be present. In this respect, the presence of other species would decrease the signal-to-noise ratio

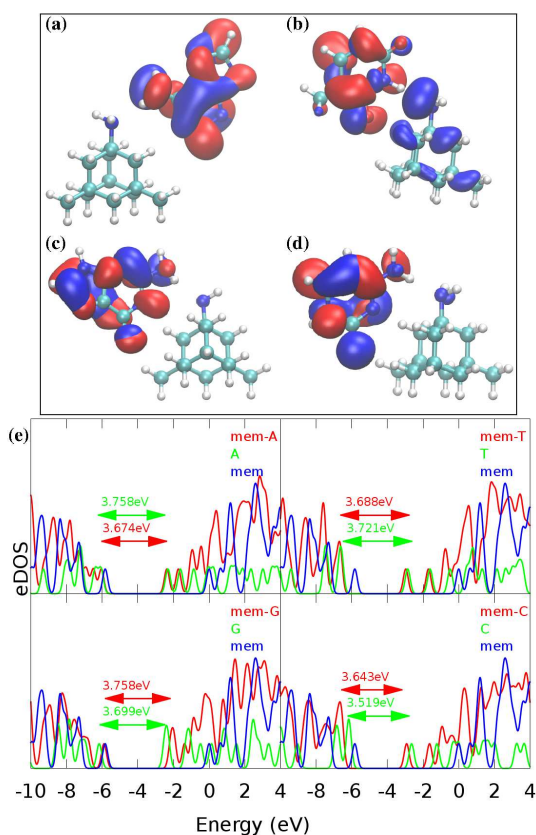


Figure 6: The frontier orbitals, HOMO (blue) and LUMO (red), for the four hydrogen bonded memantine-nucleobase complexes: (a) mem-A, (b) mem-T, (c) mem-G, and (d) mem-C. In (e) the electronic density of states (eDOS) and band gap for the memantine-nucleobases complexes are shown. The eDOS in all cases are shifted with respect to the LUMO state of amantadine which is placed at 0 eV.

of the device making the energy differences given above smaller. As a possible solution which we propose and are currently investigating are ways to further enhance the differences in the electronic properties (and as a consequence in their transport properties) of the different complexes by chemically modifying the diamondoids.

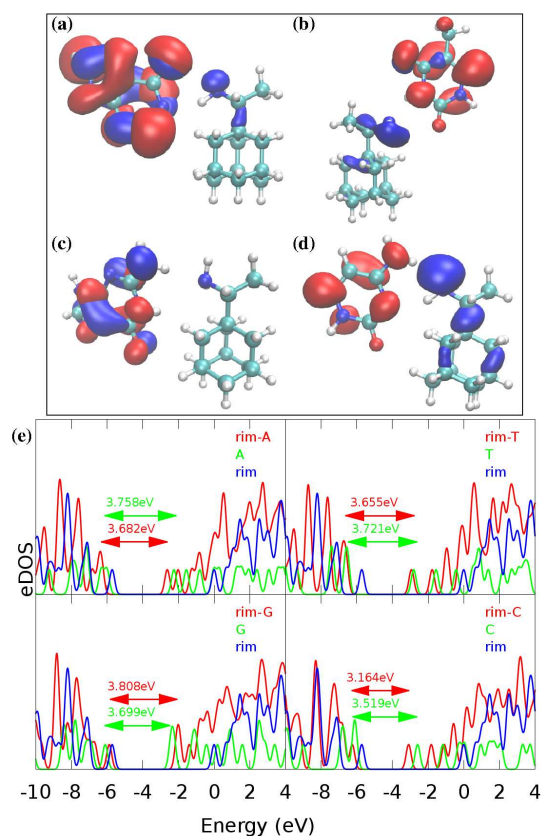


Figure 7: The frontier orbitals, HOMO (blue) and LUMO (red), for the four hydrogen bonded rimantadine-nucleobase complexes: (a) rim-A, (b) rim-T, (c) rim-G, and (d) rim-C. In (e) the electronic density of states (eDOS) and band gap for the rimantadine-nucleobases complexes are shown. The eDOS in all cases are shifted with respect to the LUMO state of amantadine which is placed at 0 eV.

Summary and conclusions

In summary, the aim of the current work was to investigate the bonding characteristics of tiny diamond clusters, the diamondoids, with nucleobases in view of potential biosensing applications. We have found, that in all cases the diamondoids tend to form hydrogen bonds with the nucleobases. The strength of the bonds are moderate, but measurable through electronic means. The bonding of the two units depends strongly on their distance and relative orientation. We have unraveled the electronic structure of the hydrogen-bonded complex by investigating the electronic band gaps, as well as the frontier orbitals of the complexes. In most cases, the main contribution in these orbitals arises from the nucleobases, while the diamondoids either do not contribute at all or are related only to the HOMO states. The differences in the electronic band gaps between the diamondoid-nucleobase complexes and the isolated nucleobases propose ways to distinguish between the nucleobases, as we have discussed in the text. We should also note here, that a wide conformational scan will be needed to examine the variation of the electronic properties for all the different distances and orientations of the diamondoid-DNA complex. This was not possible with the computational tools available in this work. It also remains to be shown how the surrounding environment in a real biosensing device will also affect the strength of the hydrogen bonds between the diamondoid-probe and the DNA molecule.

Our results are relevant to biosensing applications. We propose a biosensing device, which consists of two electrodes that are functionalized by at least one diamondoid. Regarding this functionalization, the attachment of diamondoids on metallic surfaces has been experimentally done before through thiol groups.⁷ To our knowledge, in the case of graphene or graphene nanopores, there is no relevant study. The attachment of the diamondoid on the graphene edge should depend on the terminations on the nanopore edges. Attachment could be possible by removing at one site the terminating atom and form a strong covalent C-C bond between the graphene and the diamondoid. Another possibility would be to attach the functionalizing diamondoid directly to the terminating atom, by forming a N-H bond or a C-H bond in the case of a N-terminated or H-terminated graphene sheet, respectively. Nevertheless, the attachment of a diamondoid on

graphene is not clear and would also depend on the graphene edges, whether these are zig-zag or armchair ones. We plan to look into detail on grafting possibilities of diamondoids on graphene in order to resolve these issues, prove the stability of a diamondoid-functionalized graphene pore, and propose attachment protocols for further experimental investigations.

Once the electrodes have been functionalized they are placed into a solution of biomolecules, single-stranded DNA as an example, and would potentially be able to recognize the bases using an electric field along the electrodes. A specific application we had in mind is the translocation of DNA through nanopores for ultra-fast DNA sequencing. In this case, one or additional diamondoids should functionalize the nanopore. Some of these can play the role of a *backbone-grabber* to instantly stall the biomolecule and the others play the role of the *nucleobase-reader* and sense the nucleobase.¹ These diamondoids could potentially also alternate their roles throughout the process in order to assist multiple measurements and decrease the read-out error. The choice of the size of the diamondoids will depend on the nanopore diameter. The detection will be done using transverse current measurements along the nanopore.³⁰ According to the analysis we presented on the electronic band gaps of the hydrogen bonded complexes, the different complexes should give distinguishable electronic signatures. In order to realize this, transport measurements are necessary. The use of modified diamondoids might also enhance the electronic footprint of each nucleobase in the diamondoid-nucleobase hydrogen bonded complex. Finally, it also remains to be shown, how the presence of water and ions, will affect the electronic signals and could lead to strongly distinguishable nucleobases. Work along these directions is underway.

Acknowledgement

The authors acknowledge support from the German Funding Agency (Deutsche Forschungsgemeinschaft-DFG) as part of the collaborative network SFB 716 "Dynamic simulation of systems with large particle numbers" ("Dynamische Simulation von Systemen mit großen Teilchenzahlen").

References

- (1) Branton, D. et al. *Nat. Biotechnol.* **2008**, *26*, 1146–1153.
- (2) Venkatesan, B. M.; Bashir, R. *Nat. Nanotechnol.* **2011**, *6*, 615–624.
- (3) Wanunu, M. *Phys. Life Rev.* **2012**, *9*, 125–158.
- (4) Miles, B. N.; Ivanov, A. P.; Wilson, K. A.; Dogan, F.; Japrun, D.; Edel, J. B. *Chem. Soc. Rev.* **2013**, *42*, 15–28.
- (5) He, H.; Scheicher, R. H.; Pandey, R.; Rocha, A. R.; Sanvito, S.; Grigoriev, A.; Ahuja, R.; Karna, S. P. *J. Phys. Chem. C* **2008**, *112*, 3456–3459.
- (6) Marchand, A. P. *Science* **2003**, *299*.
- (7) Yang, W. L. et al. *Science* **2007**, *316*, 1460–1462.
- (8) Wang, Y.; Kioupakis, E.; Lu, X.; Wegner, D.; Yamachika, R.; Dahl, J. E.; Carlson, R. M. K.; Louie, S. G.; Crommie, M. F. *Nat. Mater.* **2008**, *7*, 38–42.
- (9) Zhang, G. *Phys. Today* **2013**, *66*, 59–60.
- (10) Huang, H.; Pierstorff, E.; Osawa, E.; Ho, D. *Nano. Lett.* **2007**, *7*, 3305–3314.
- (11) Stouffer, A. L.; Acharya, R.; Salom, D.; Levine, A. S.; Costanzo, L. D.; Soto, C. S.; Tereshko, V.; Nanda, V.; Stayrook, S.; DeGrado, W. F. *Nature* **2008**, *451*.
- (12) Spasov, A. A.; Khamidova, T. V.; Bugaeva, L. I.; Morozov, I. *Pharm. Chem. J.* **2000**, *34*, 1–7.
- (13) Schnell, J. R.; Chou, J. J. *Nature* **2008**, *451*, 591–595.
- (14) Geldenhuys, W. J.; Malan, S. F.; Bloomquist, J. R.; Marchand, A. P.; der Schyf, C. J. V. *Med. Res. Rev.* *25*, 21–48.
- (15) Xue, Y.; Mansoori, G. A. *Int. J. Nanosci.* **2008**, *7*, 63–72.

- (16) Drummond, N.D.; Williamson, A.J.; Needs, R.J. and Galli, G. *Phys. Rev. Lett.* **2008**, *95*, 096801.
- (17) Landt, L.; Bostedt, C.; Wolter, D.; Möller, T.; Dahl, J. E. P.; Carlson, R. M. K.; Tkachenko, B. A.; Fokin, A. A.; Schreiner, P. R.; Kulesza, A.; Mitric, R.; Bonacic-Koutecky, V. *J. Chem. Phys.* **2010**, *132*, 144305.
- (18) Landt, L.; Staiger, M.; Wolter, D.; Klunder, K.; Zimmermann, P.; Willey, T. M.; van Buren, T.; Brehmer, D.; Schreiner, P. R.; Tkachenko, B. A.; Fokin, A. A.; Moller, T.; Bostedt, C. *J. Chem. Phys.* **2010**, *132*, 024710.
- (19) Rander, T.; Staiger, M.; Richter, R.; Zimmermann, T.; Landt, L.; Wolter, D.; Dahl, J.E.; Carlson, M.K.; Tkachenko, B. A.; Fokina, N.A.; Schreiner, P. R.; Moller, T.; Bostedt, C. *J. Chem. Phys.* **2013**, *138*, 024310.
- (20) Soler, J. M.; Artacho, E.; Gale, J. D.; García, A.; Junquera, J.; Ordejón, P.; Sánchez-Portal, D. *J. Phys.-Condens. Mat.* **2002**, *14*, 2745–2779.
- (21) Troullier, N.; Martins, J. L. *Phys. Rev. B* **1991**, *43*, 1993–2006.
- (22) Junquera, J.; Paz, O.; Sánchez-Portal, D.; Artacho, E. *Phys. Rev. B* **2001**, *64*, 235111.
- (23) Lee, K.; Murray, E. D.; Kong, L.; Lundqvist, B. I.; Langreth, D. C. *Phys. Rev. B* **2010**, *82*, 081101(R).
- (24) Klimeš, J.; Michaelides, A. *J. Chem. Phys.* **2012**, *137*, 120901.
- (25) Šponer, J.; Jurečka, P.; Hobza, P. *J. Am. Chem. Soc.* **2004**, *126*, 10142–10151.
- (26) Cooper, V. R.; Thonhauser, T.; Langreth, D. C. *J. Chem. Phys.* **2008**, *128*, 204102.
- (27) Boys, S. F.; Bernardi, F. *Mol. Phys.* **1970**, *19*, 553–566.
- (28) Ireta, J.; Neugebauer, J.; Scheffler, M. *J. Phys. Chem. A* **2004**, *108*, 5692–5698.

- (29) Steiner, T. *Angew. Chem. Int. Ed.* **2002**, *41*.
- (30) Zwolak, M.; Di Ventra, M. *Rev. Mod. Phys.* **2008**, *80*, 141-165.

